

Diversity of Coordination Modes in a Flexible Ditopic Ligand Containing 2-pyridyl, Carbonyl and Hydrazone Functionalities: Mononuclear and Dinuclear Cobalt(III) Complexes, and Tetranuclear Copper(II) and Nickel(II) Clusters[†]

Evangelos Pilichos ¹, Evangelos Spanakis ¹, Evangelia-Konstantina Maniaki ¹, Catherine P. Raptopoulou ², Vassilis Psycharis ^{2,*}, Mark M. Turnbull ^{3,*} and Spyros P. Perlepes ^{1,4,*}

¹ Department of Chemistry, University of Patras, 26504 Patras, Greece; pilvag@gmail.com (E.P.); veespan92@gmail.com (E.S.); evitamaniaki@yahoo.gr (E.K.M.)

² Institute of Nanoscience and Nanotechnology, NCSR “Demokritos”, 15310 Aghia Paraskevi Attikis, Greece; c.raptopoulou@inn.demokritos.gr

³ Carlson School of Chemistry and Biochemistry, Clark University, Worcester, MA, USA

⁴ Institute of Chemical Engineering Sciences, Foundation for Research and Technology-Hellas (FORTH/ICE-HT), Platani, B.O. Box 1414, 26504 Patras, Greece

* Correspondence: v.psycharis@inn.demokritos.gr (V.P.); MTurnbull@clarku.edu (M.M.T.); perlepes@patreas.upatras.gr (S.P.P.); Tel.: +30-210-6503346 (V.P.); +1-508-7937167(M.M.T); +30-2610-996730 (S.P.P.)

[†] This article is dedicated to Professor Masahiro Yamashita-a great scientist and a precious friend-on the occasion of his 65th birthday.

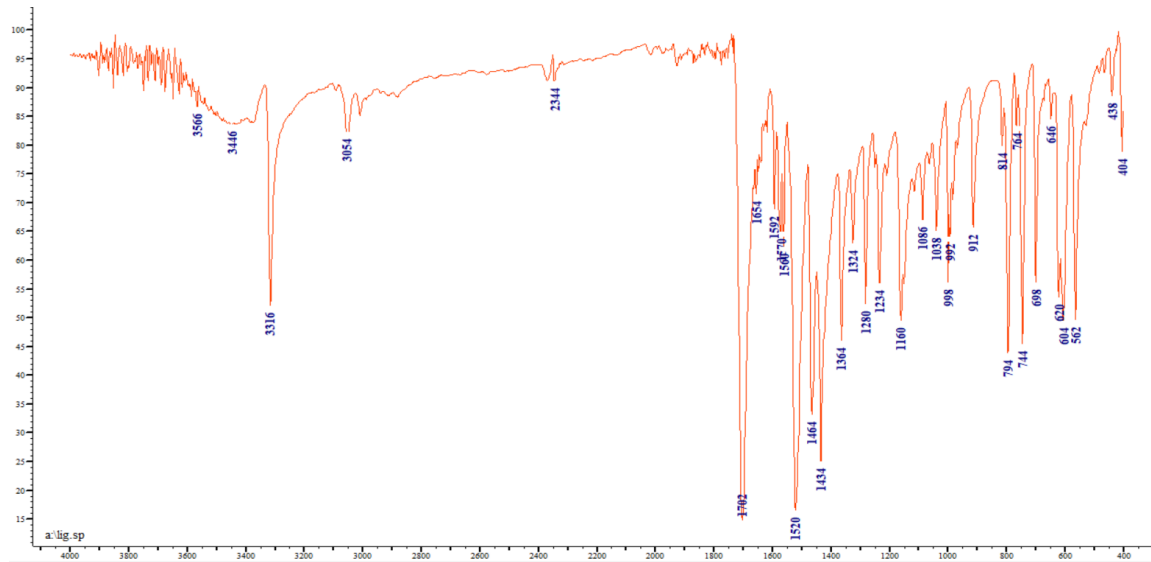


Figure S1. The IR spectrum (KBr, cm^{-1}) of the free ligand LH.

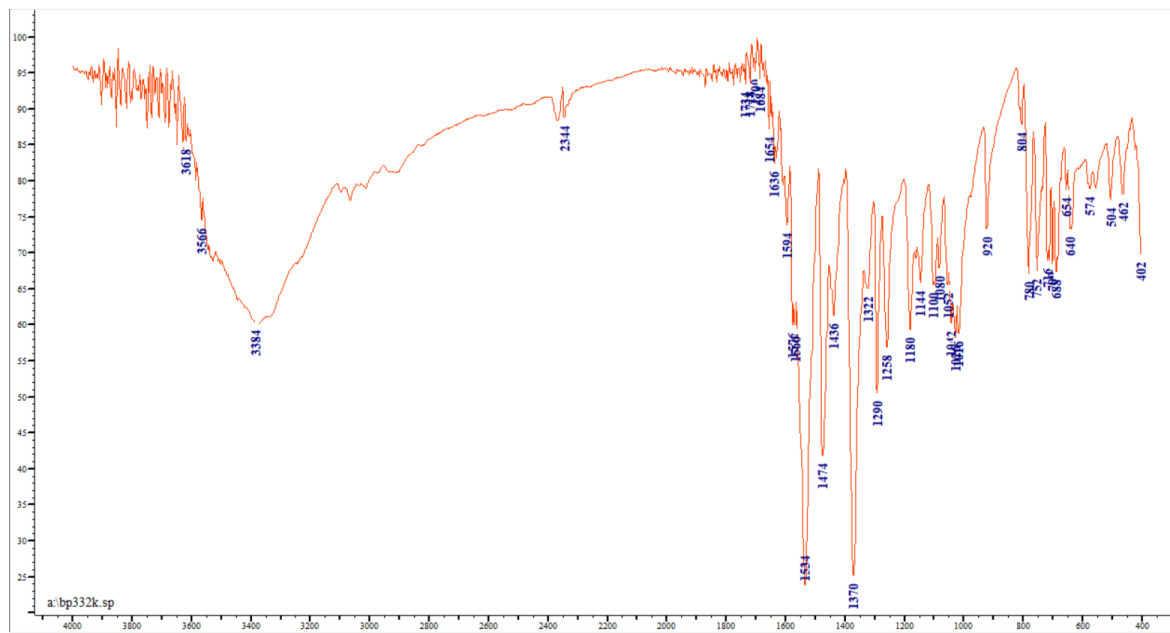


Figure S2. The IR spectrum (KBr, cm⁻¹) of sample **1**. The broad band at 3384 cm⁻¹ is due to humidity.

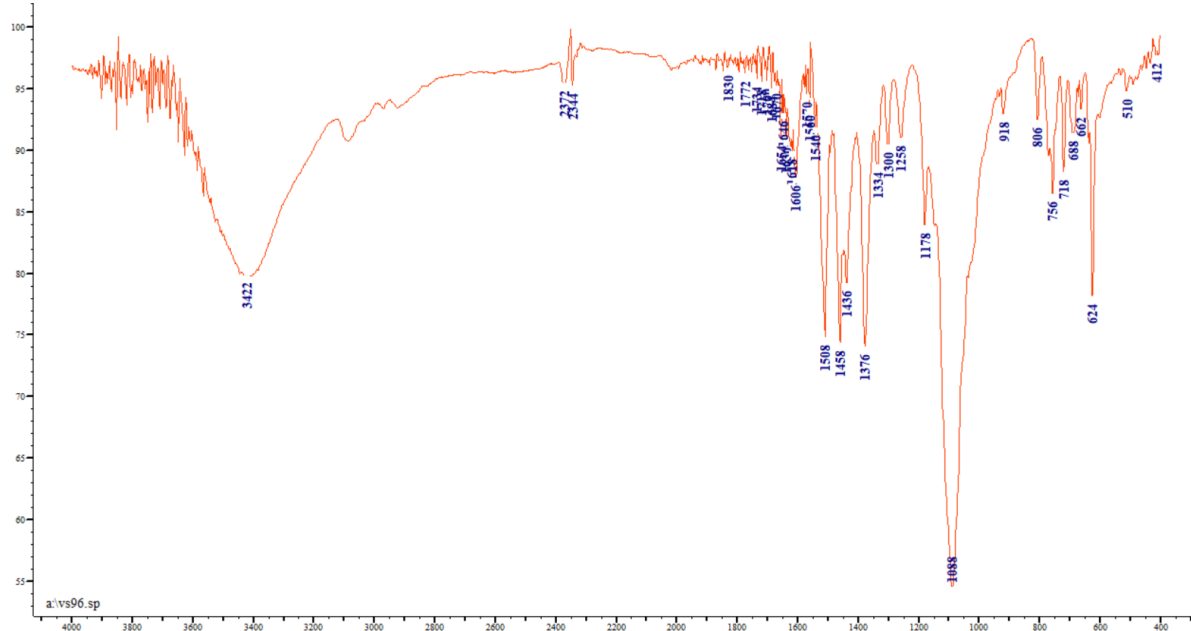


Figure S3. The IR spectrum (KBr, cm⁻¹) of sample **3·H₂O**.

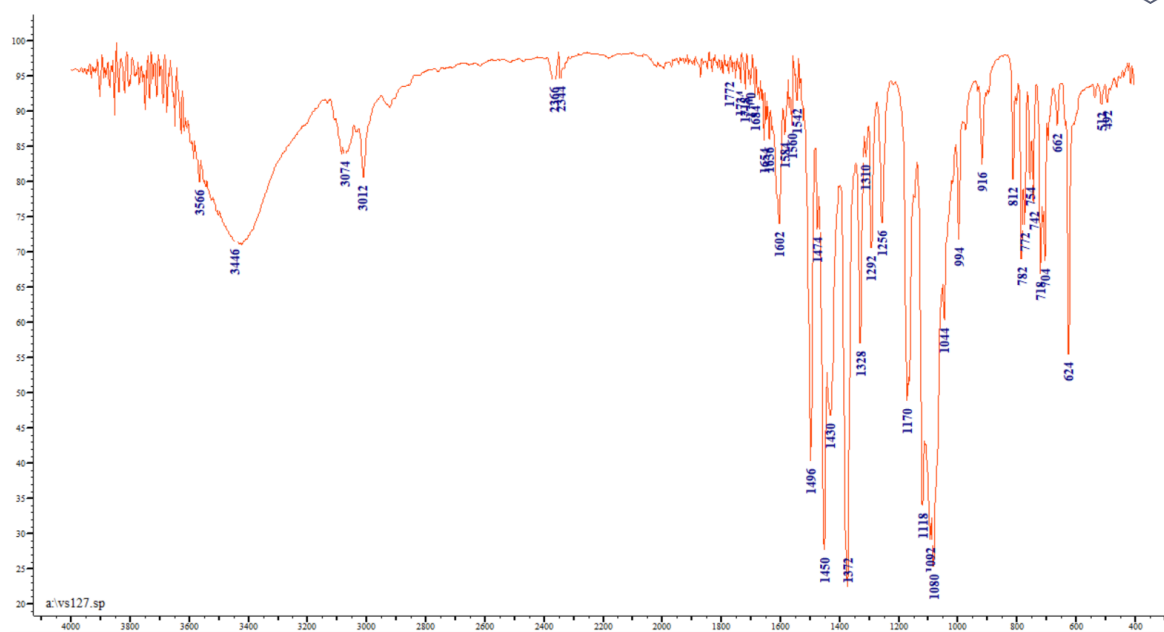


Figure S4. The IR spectrum (KBr, cm⁻¹) of complex 4. The broad band at 3446 cm⁻¹ is due to humidity.

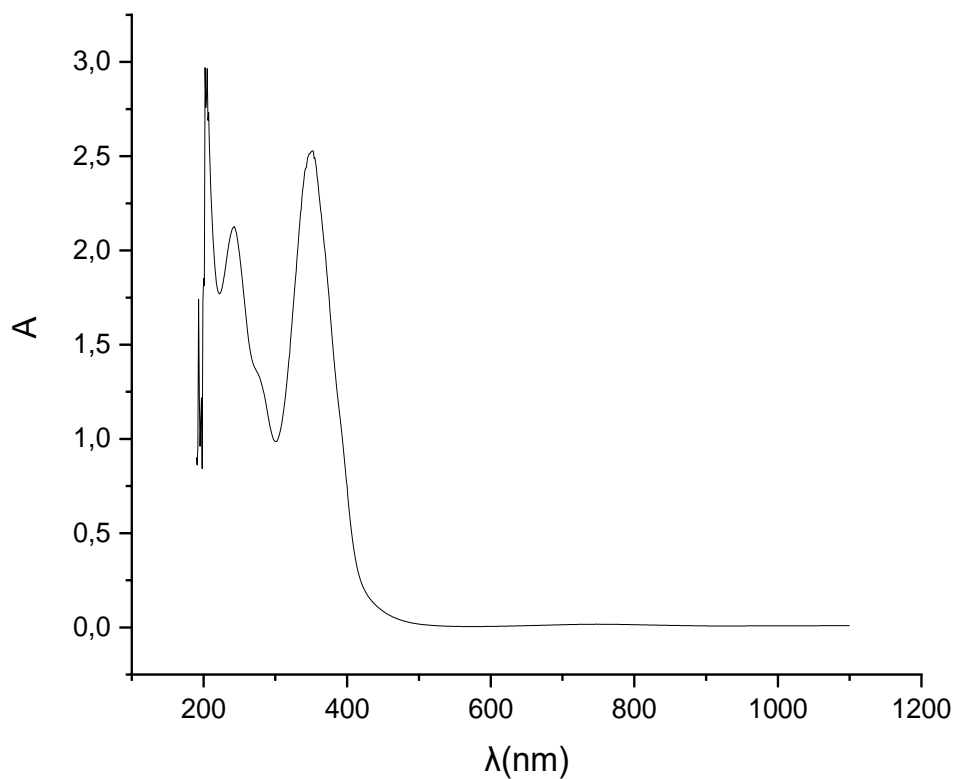


Figure S5. The UV/VIS/Near-IR spectrum (nm) of sample 1 in MeOH.

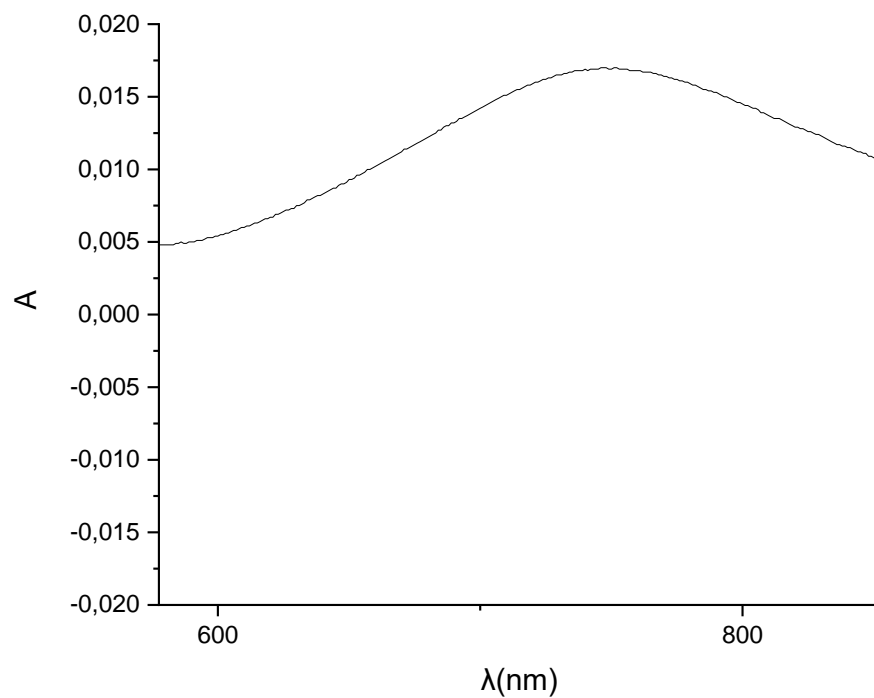
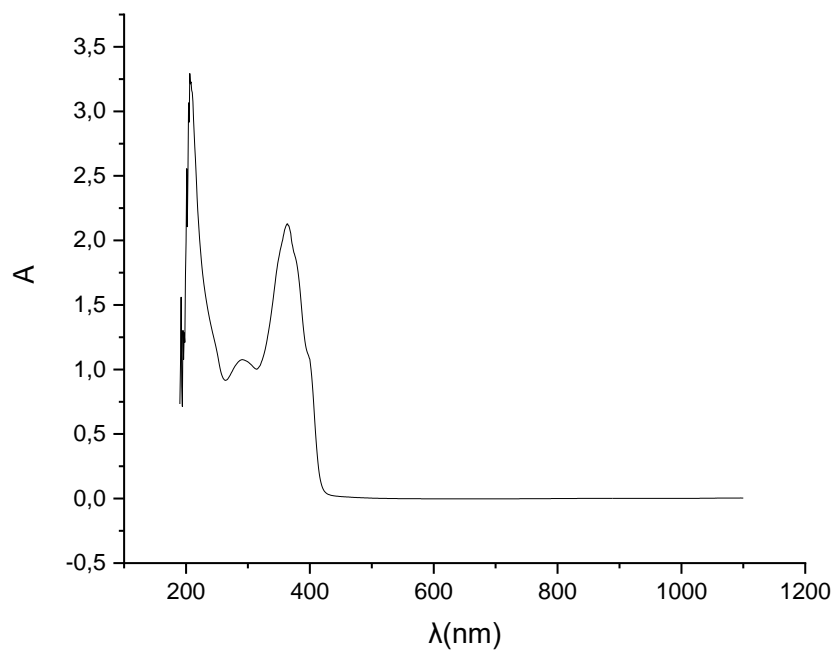


Figure S6. The VIS spectrum (nm) of sample **1** in MeOH.



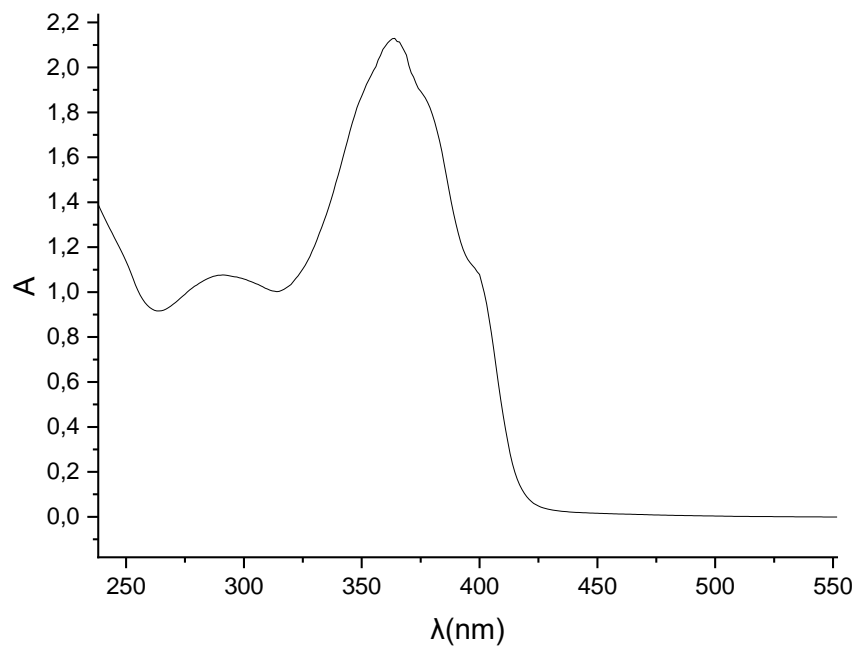


Figure S7. UV/VIS/Near-IR spectra (nm) of sample **2** in MeOH.

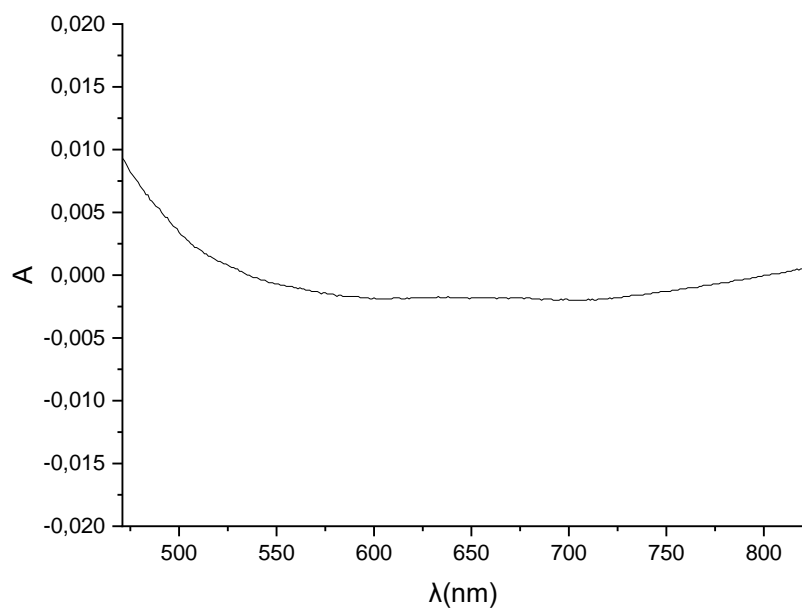


Figure S8. The VIS spectrum (nm) of sample **2** in MeOH.

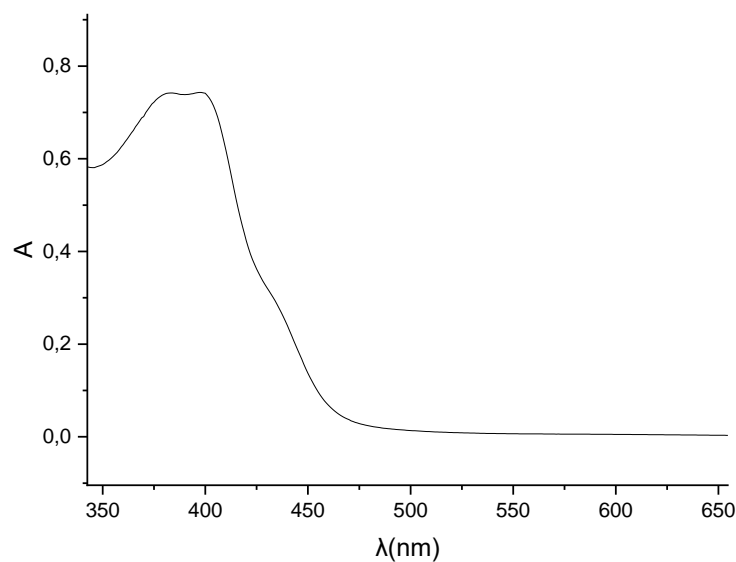
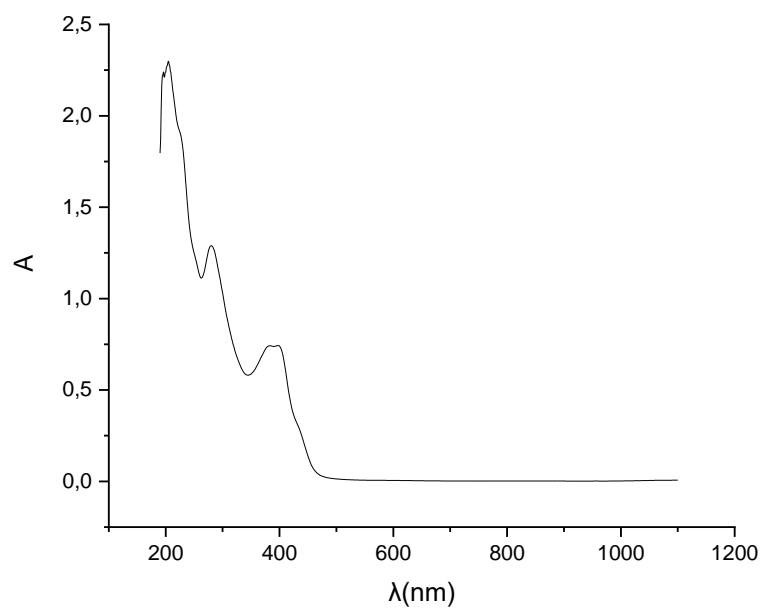


Figure S9. UV/VIS/Near-IR spectra (nm) of sample $3 \cdot H_2O$ in MeCN.

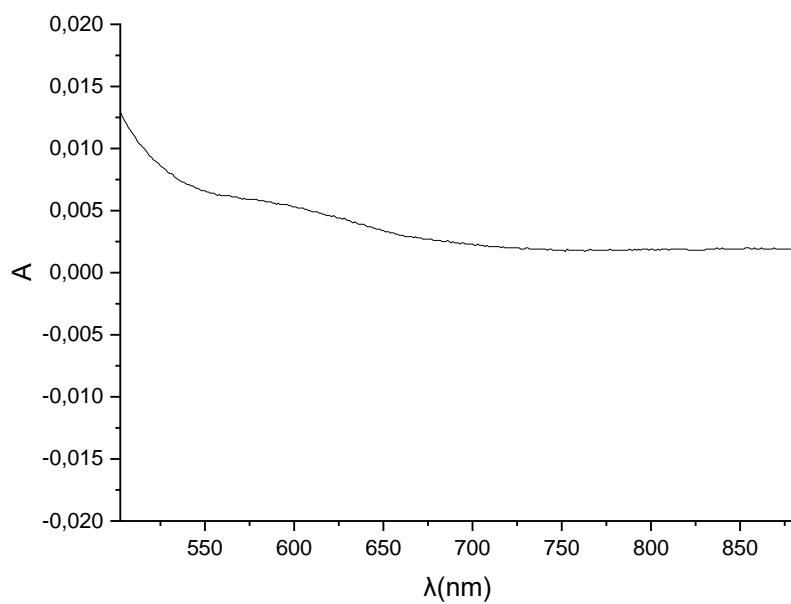
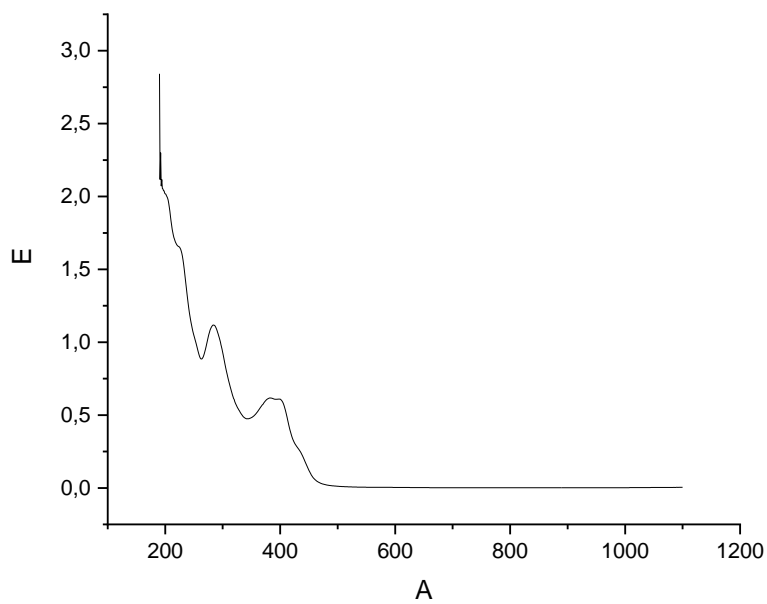


Figure S10. The VIS spectrum (nm) of sample **3·H₂O** in MeCN.



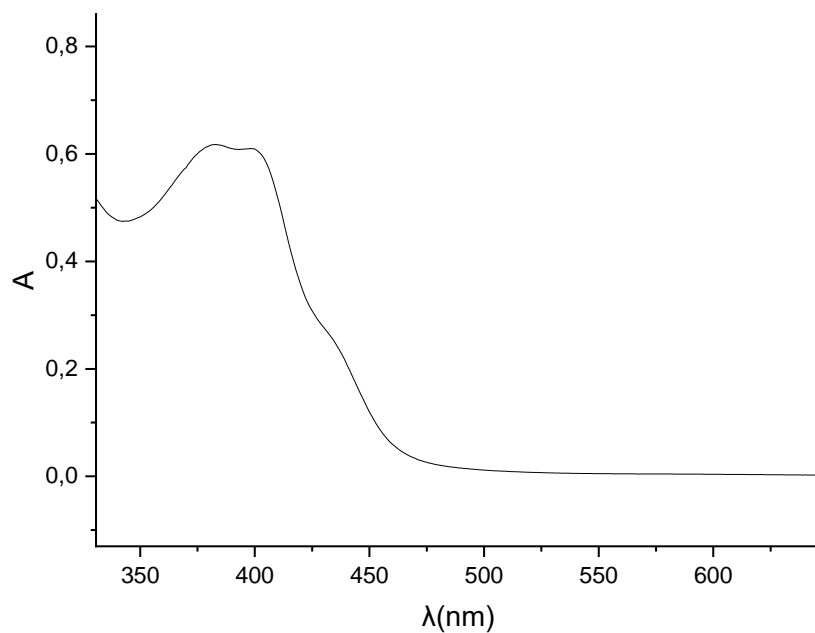


Figure S11. UV/VIS/Near-IR spectra (nm) of complex **4** in MeCN.

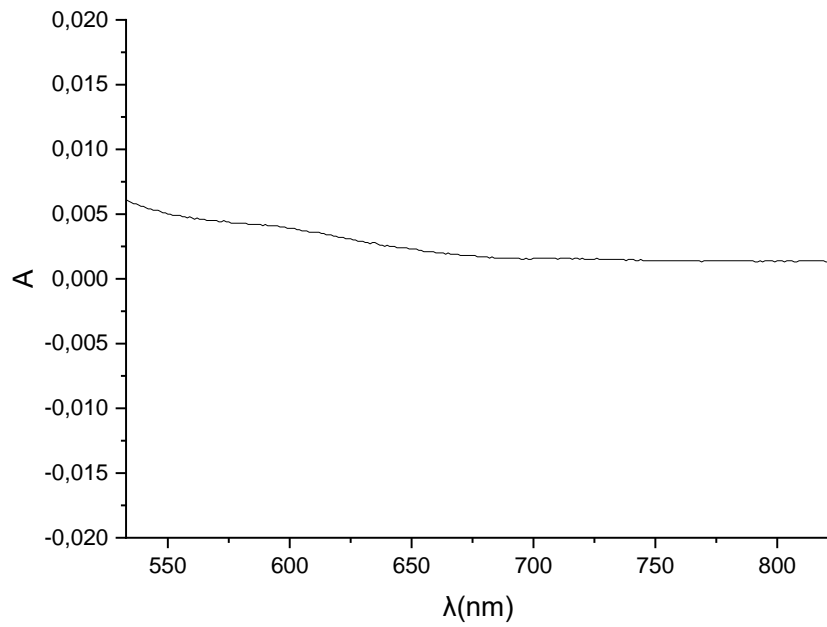


Figure S12. The VIS spectrum (nm) of complex **4** in MeCN.

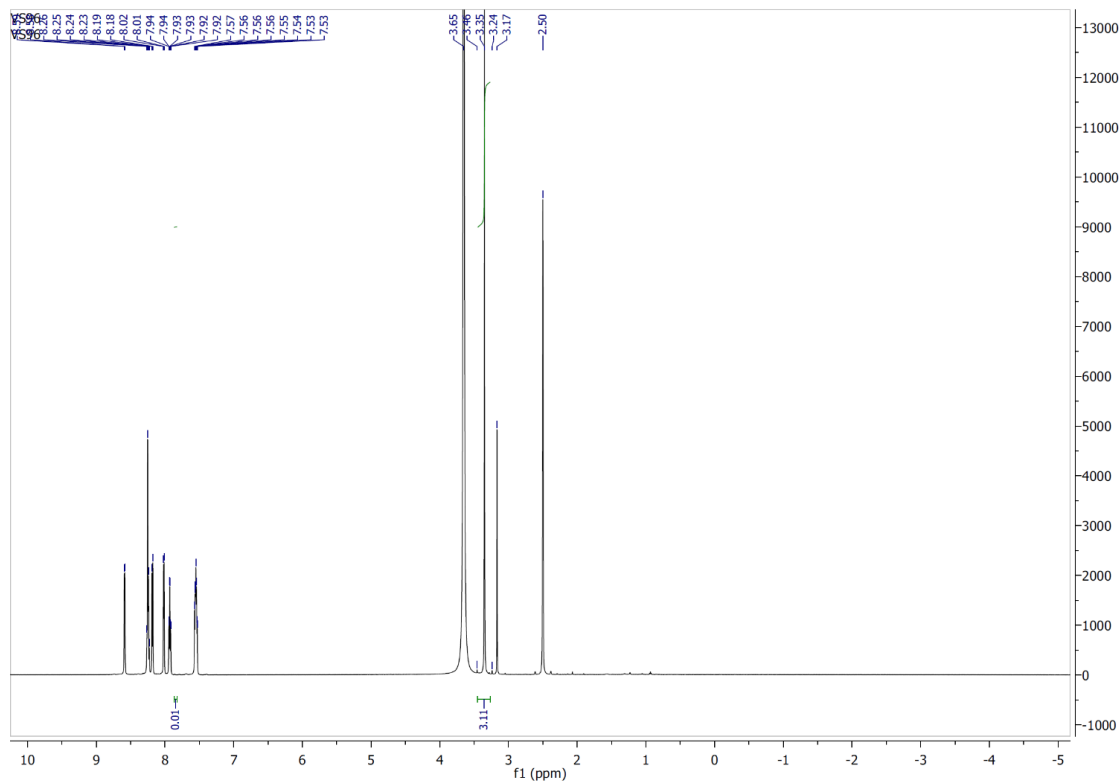


Figure S13. The ¹H NMR spectrum (DMSO-d₆, δ/ ppm) of sample 3·H₂O. The peak at δ 2.50 ppm is due to the methyl protons of the non-deuterated percentage of the solvent.

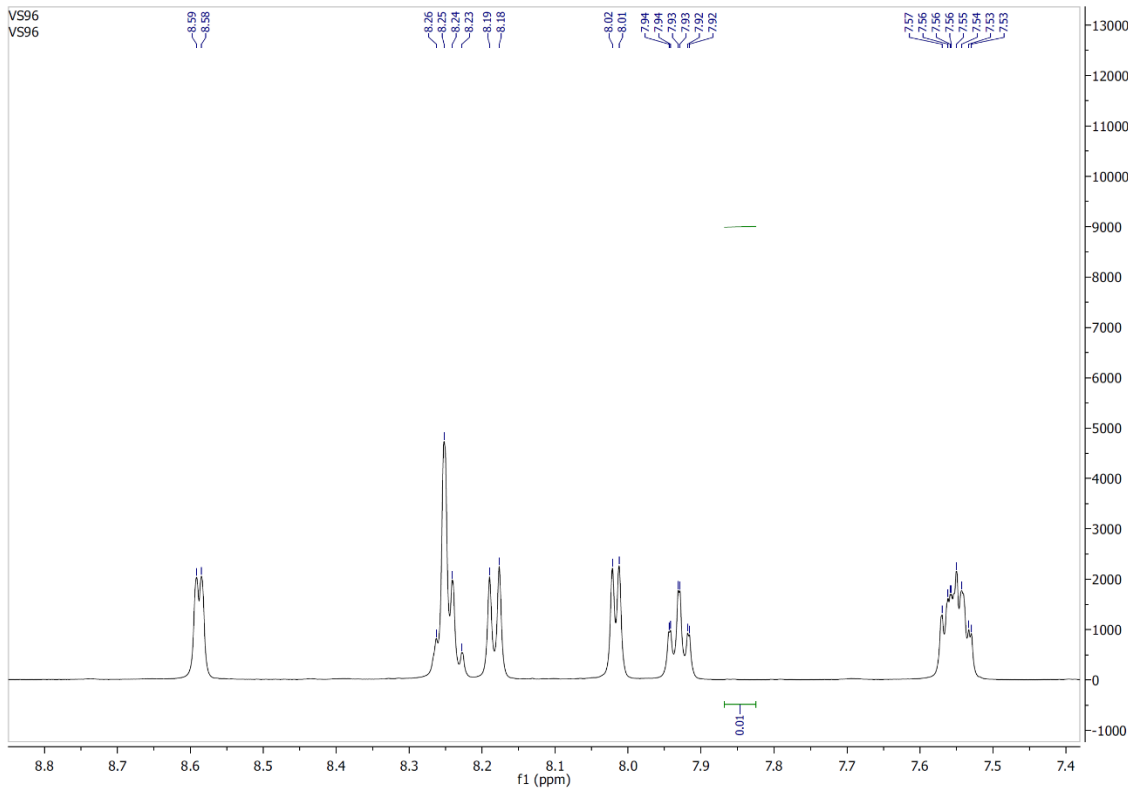


Figure S14. The aromatic region in the ¹H NMR spectrum (DMSO-d₆, δ/ ppm) of sample 3·H₂O.

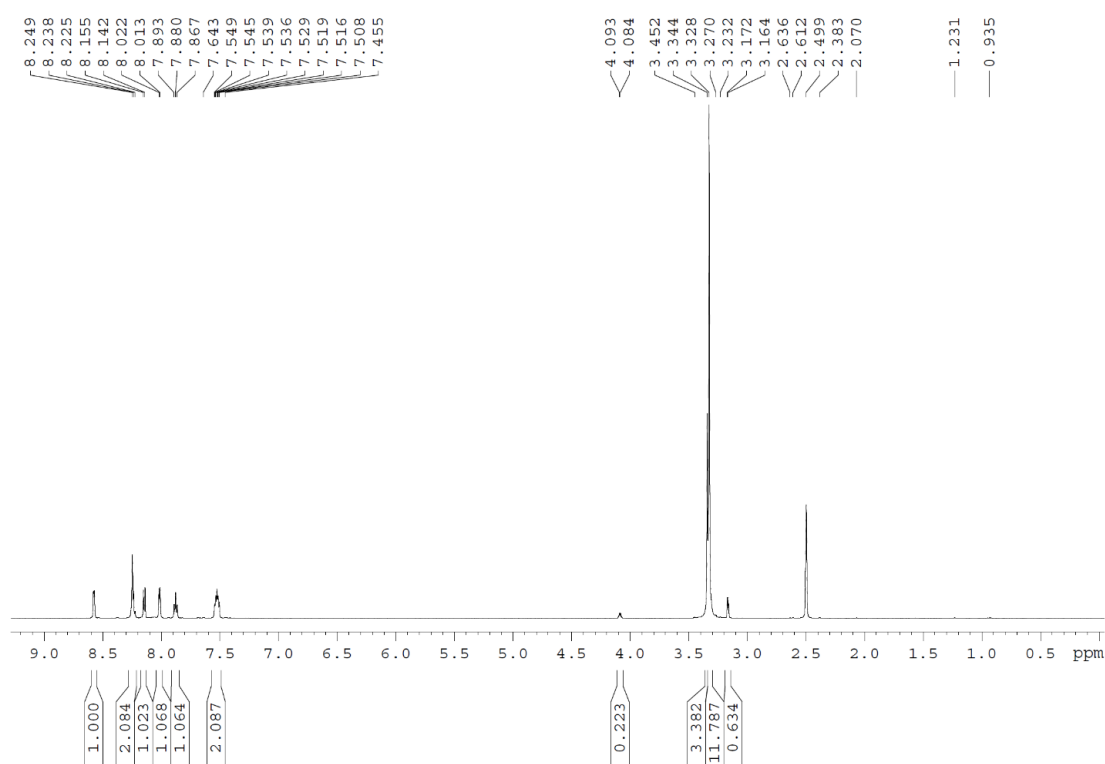


Figure S15. The ¹H NMR spectrum (DMSO-d₆, δ /ppm) of complex 4. The peak at δ 2.50 ppm is due to the methyl protons of the non-deuterated percentage of the solvent.

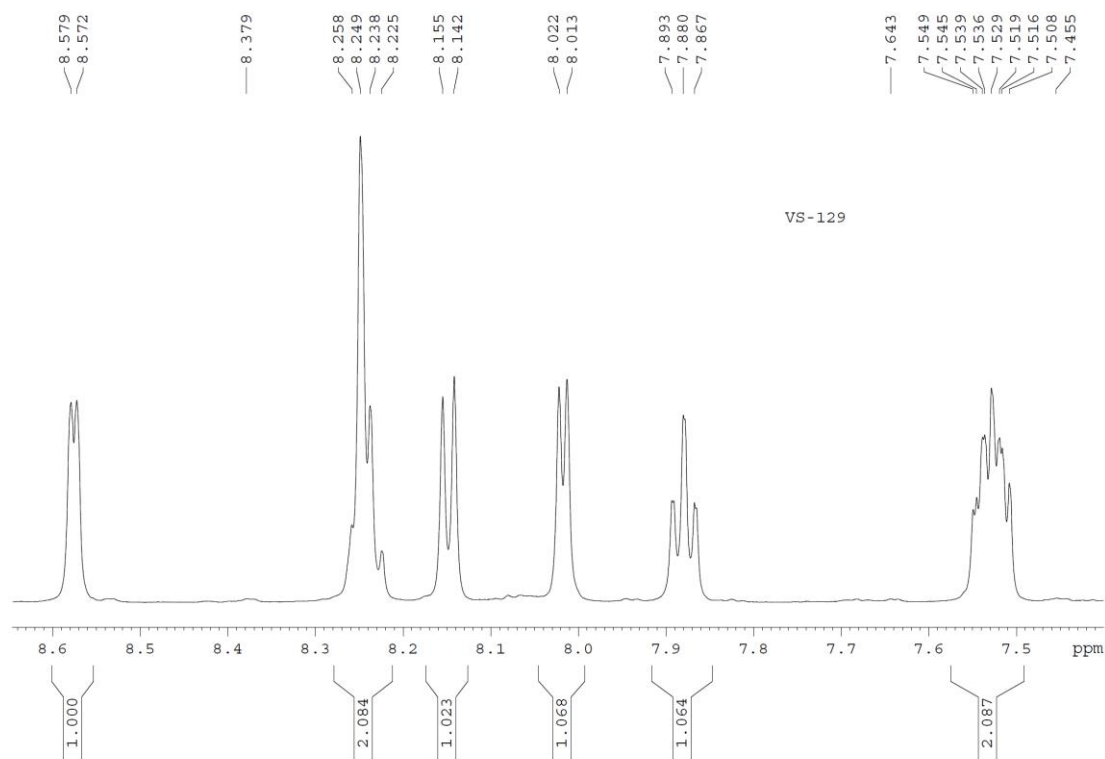


Figure S16. The aromatic region in the ¹H NMR spectrum (DMSO-d₆, δ /ppm) of complex 4.

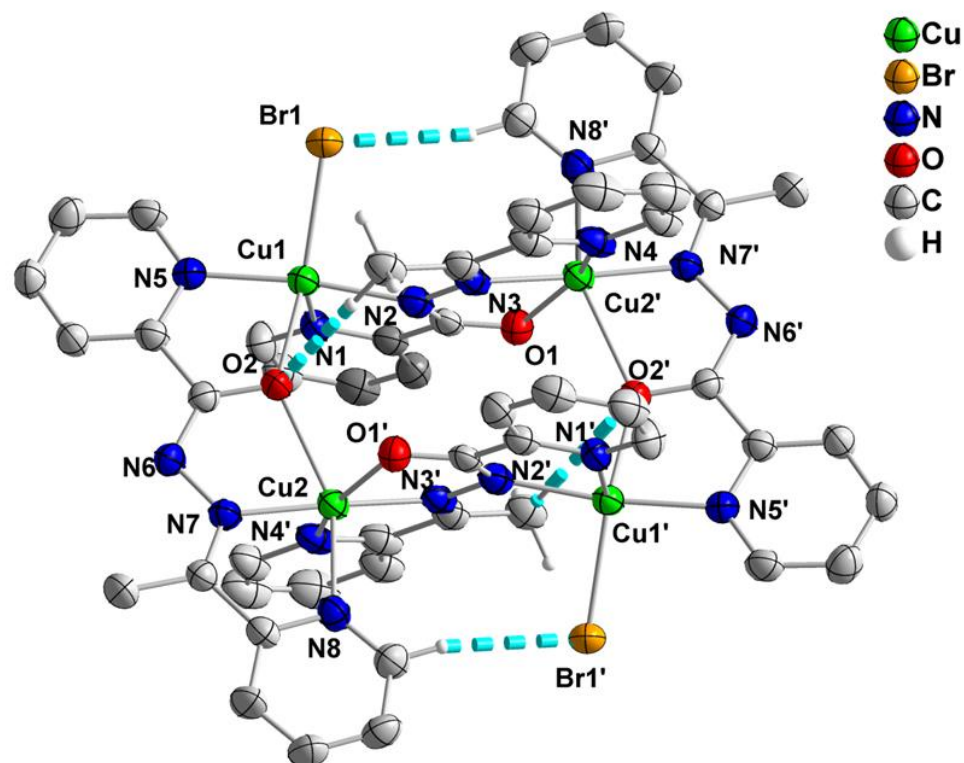


Figure S17. Partially labelled ORTEP plot of the tetranuclear cation $[\text{Cu}_4\text{Br}_2(\text{L})_4]^{2+}$ that is present in the crystal structure of $\mathbf{1} \cdot 0.8\text{H}_2\text{O} \cdot \text{MeOH}$. Thermal ellipsoids are presented at the 50% probability level. The figure also shows the intracationic H bonds (dashed thick cyan lines). Symmetry code: $(') = -x+1, -y+2, -z$.

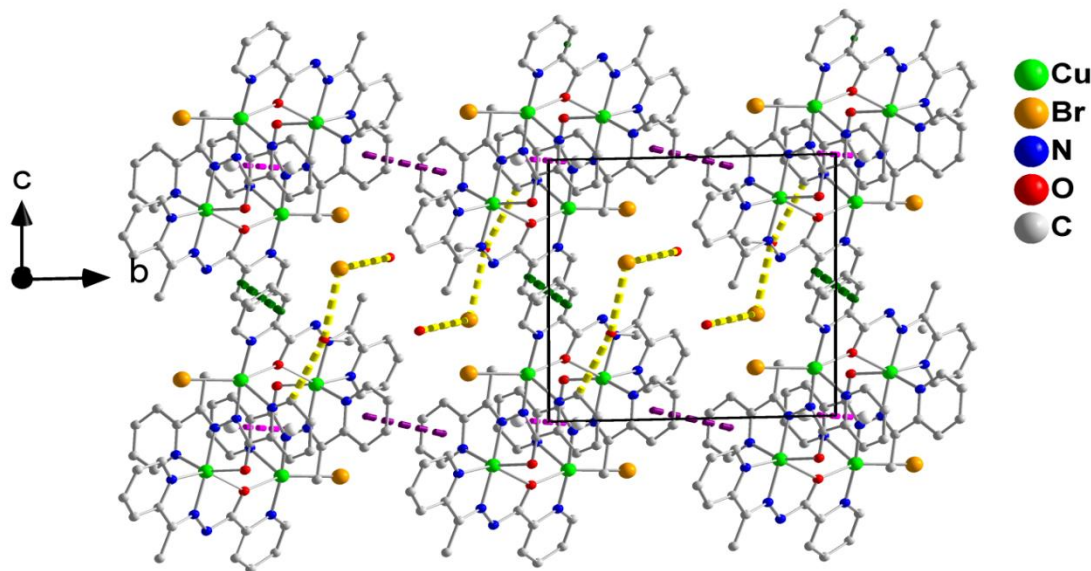


Figure S18. A portion of the 3D arrangement of complex $\mathbf{1} \cdot 0.8\text{H}_2\text{O} \cdot \text{MeOH}$. The dashed green lines indicate the $\pi-\pi$ interactions between centrosymmetrically-related ligands involving the N5,N8-containing rings that belong to adjacent layers. The dashed yellow lines represent H bonds involving the Br⁻ counterions and the solvent MeOH molecules that are hosted in the lattice. The color code for the pink and violet lines is the same with that used in Figure 2.

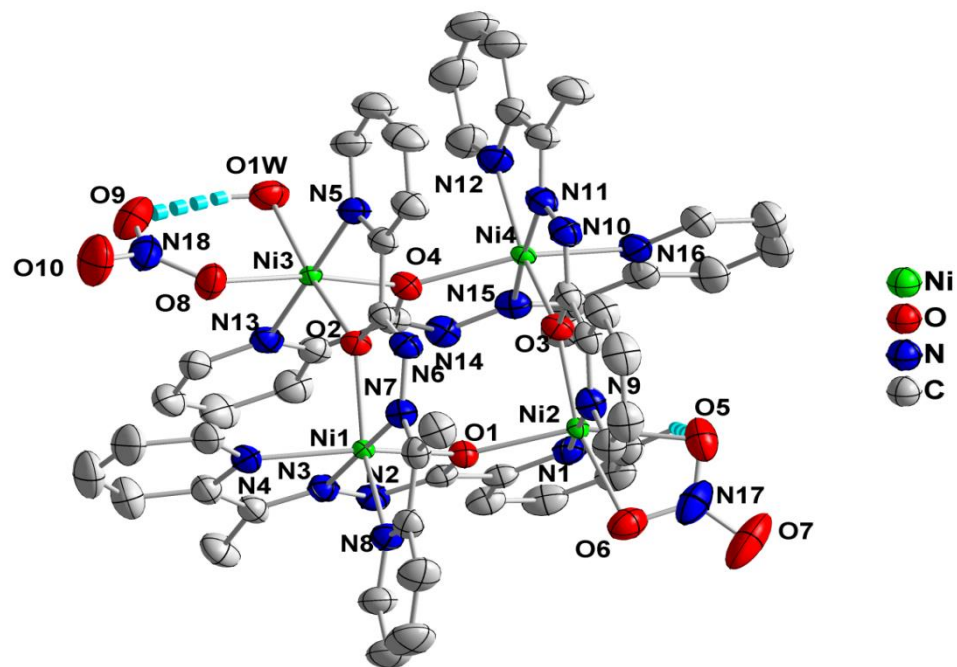


Figure S19. Partially labelled ORTEP plot of the tetranuclear cation $[\text{Ni}_4(\text{NO}_3)_2(\text{L})_4(\text{H}_2\text{O})]^{2+}$ that is present in the crystal structure of **2**·0.2H₂O·3EtOH. Thermal ellipsoids are presented at the 50% probability level. The figure also shows the intracationic H bonds (dashed thick cyan lines).

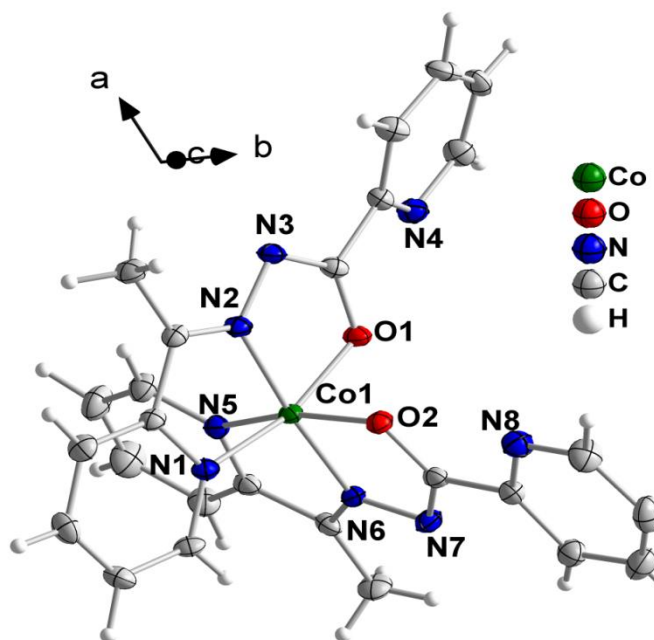


Figure S20. Partially labelled ORTEP plot of the mononuclear cation $[\text{Co}(\text{L})_2]^{+}$ that is present in the crystal structure of **4**.

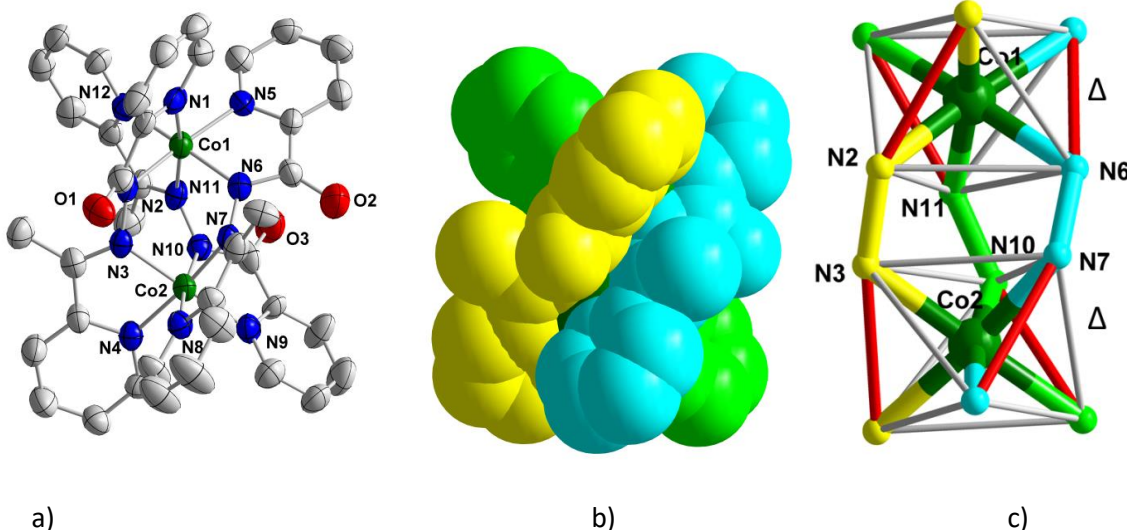


Figure S21. a) Partially labelled ORTEP plot of the dinuclear cation $[\text{Co}_2(\text{L})_3]^{3+}$ that is present in the crystal structure of $\mathbf{3} \cdot 0.8\text{H}_2\text{O} \cdot 1.3\text{MeOH}$; thermal ellipsoids are presented at the 50% probability level. b) Space filling representation of the three coordinated ligands in the cation $[\text{Co}_2(\text{L})_3]^{3+}$; ligands possessing O1, O2 and O3 are indicated with yellow, cyan and green colors, respectively. c) Polyhedral representation of the coordination spheres of the cation of $\mathbf{3} \cdot 0.8\text{H}_2\text{O} \cdot 1.3\text{MeOH}$ revealing the Δ,Δ ‘right-handed’ character of the shown, helicate-type cation.

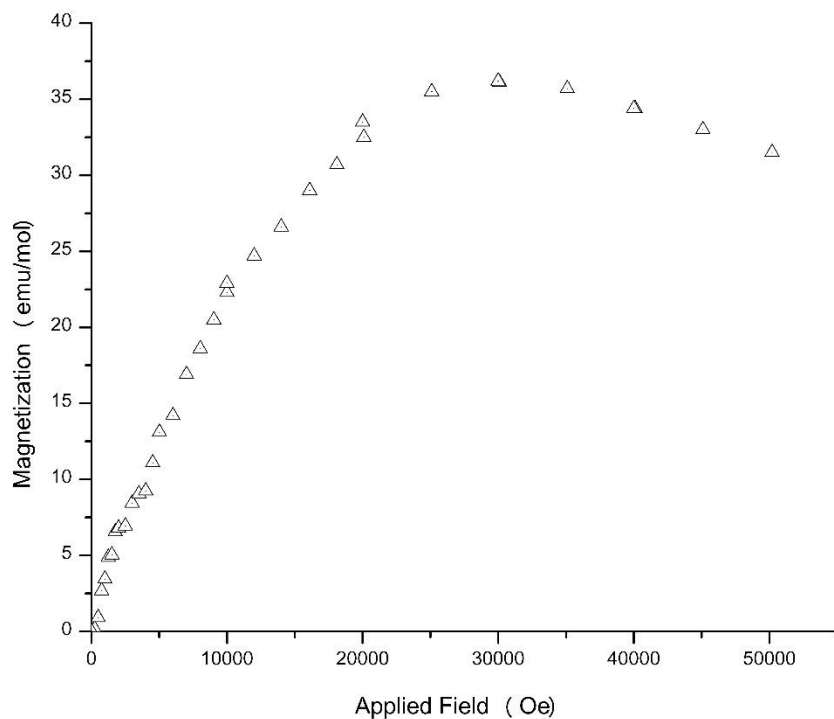


Figure S22. Magnetization as a function of applied field for $\mathbf{1}$ at 1.8 K. The slight downturn above 30 kOe results from saturation of the trace paramagnetic impurity and subsequent increase in the diamagnetic response of the sample with increasing field.

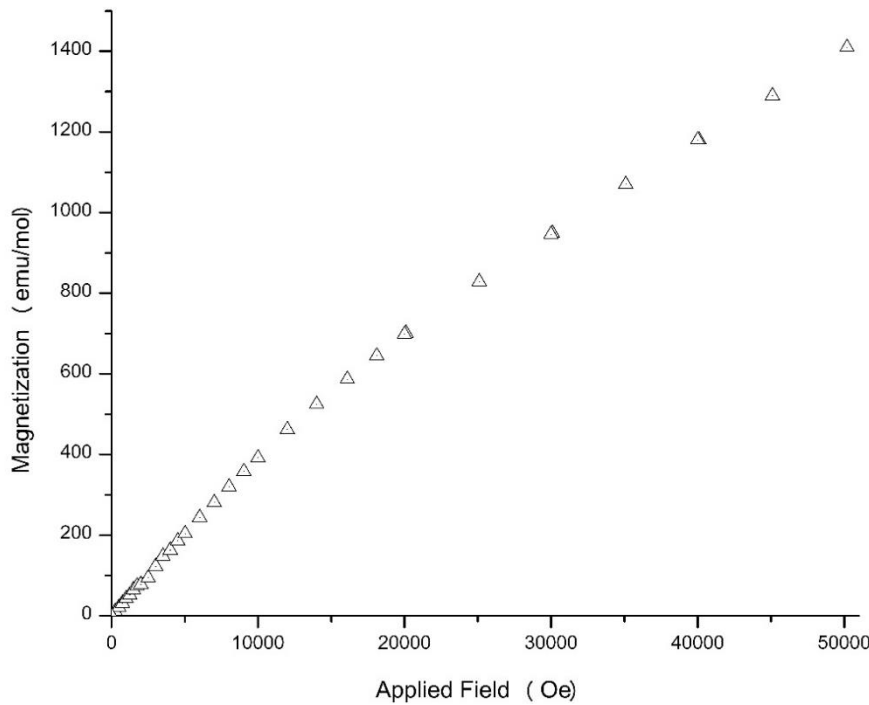


Figure S23. Magnetization as a function of applied field for **2** at 1.8 K.

Table S1. Crystallographic data for complexes **1**·0.8H₂O·MeOH, **2**·0.2H₂O·3EtOH, **3**·0.8H₂O·1.3MeOH and **4**.

Parameter	1 ·0.8H ₂ O·MeOH	2 ·0.2H ₂ O·3EtOH	3 ·0.8H ₂ O·1.3MeOH	4
Formula	C ₅₃ H _{49.60} N ₁₆ Cu ₄ O _{5.80} Br ₄	C ₅₈ H _{64.40} N ₂₀ Ni ₄ O _{20.20}	C _{40.30} H _{39.80} Ni ₂ Co ₂ O _{17.10} Cl ₃	C ₂₆ H ₂₂ N ₈ CoO ₆ Cl
Formula weight	1577.28	1599.73	1190.05	636.89
Crystal system	triclinic	triclinic	monoclinic	triclinic
Space group	P $\bar{1}$	P $\bar{1}$	C $2/c$	P $\bar{1}$
Radiation	Mo K α	Mo K α	Cu K α	Cu K α
T/K	170	170	160	170
a/ \AA	11.4305(5)	13.1227(2)	22.5881(6)	8.8881(2)
b/ \AA	11.8331(5)	14.6639(3)	13.6462(4)	11.2130(2)
c/ \AA	12.0675(4)	19.8993(4)	31.8078(8)	15.0214(3)
$\alpha/^\circ$	85.761(1)	101.240(1)	90.00	103.237(1)
$\beta/^\circ$	74.357(1)	108.445(1)	94.684(3)	103.941(1)
$\gamma/^\circ$	78.428(1)	96.165(1)	90.00	105.571(1)
V/ \AA^3	1539.48(11)	3503.52(12)	9771.7(5)	1328.81(5)
Z	1	2	8	2
D _{calcd} /g cm ⁻³	1.701	1.516	1.618	1.592
μ/mm^{-1}	4.02	1.14	7.57	6.50
2 $\theta_{\text{max}}/^\circ$	52.0	54.0	125.0	130.0
Reflections collected	25834	65892	29038	17420
Reflections unique (R_{int})	5982(0.069)	15261(0.032)	7436(0.074)	4401(0.049)
Reflections with $I > 2\sigma(I)$	4164	11942	4420	3990

No. of parameters	391	1076	763	467
$R_1^a [I > 2\sigma(I)]$	0.0580	0.0442	0.0803	0.0429
wR_2^b (all data)	0.1704	0.1332	0.2181	0.1034
GOF(F^2)	1.09	1.05	1.03	1.12
$\Delta\rho_{\max}/\Delta\rho_{\min}$ (e Å ⁻³)	1.64/-1.09	1.07/-0.62	0.53/-0.45	0.58/-0.55
CCDC				

^a $R_1 = \sum(|F_o| - |F_c|)/\sum(|F_o|)$; ^b $wR_2 = \{\sum[w(F_o^2 - F_c^2)]/\sum[w(F_o^2)^2]\}^{1/2}$, with $w =$

$1/[\sigma^2(F_o^2) + (aP)^2 + (bP)]$, where $P = (F_o^2 + 2F_c^2)/3$ [a = 0.0902 and b = 1.4142 for **1**·0.8H₂O·MeOH, a = 0.0758 and b = 2.1977 for **2**·0.2H₂O·3EtOH, a = 0.1106 and b = 21.3349 for **3**·0.8H₂O·1.3MeOH, a = 0.0448 and b = 0.6972 for **4**].

Table S2. Crystallographically independent H-bonding interactions in the crystal structure of cluster **1**·0.8H₂O·MeOH.^{a,b}

D-H···A	D-H (Å)	H···A (Å)	D···A (Å)	D-H···A (°)
C7-H _A (C7)···O2	0.98	2.42	3.389(8)	170
C26-H(C26)···Br1 ⁱ	0.95	2.82	3.739(7)	164
O1M-H(O1M)···Br2 ⁱⁱ	0.82	2.65	3.359(6)	145.9
C1-H(C1)···O1M ⁱⁱⁱ	0.95	2.44	3.283(9)	148

^a C7 is a methyl carbon atom, C1 and C6 are aromatic carbon atoms, O1M is the oxygen atom of the MeOH lattice molecule, and Br2 is the bromide counterion; all these atoms are not shown or/and labelled in Figures 1 and S17. ^b Symmetry codes: (i) $-x+1, -y+2, -z$; (ii) $-x+1, -y+1, -z+1$; (iii) $x, y+1, z$. D = donor; A = acceptor.

Table S3. H-bonding interactions in the crystal structure of cluster **2**·0.2H₂O·3EtOH.^{a,b}

D-H···A	D-H (Å)	H···A (Å)	D···A (Å)	D-H···A (°)
Intracationionic Interactions				
O1W-H _B (O1W)···O9	0.81(4)	1.88(4)	2.657(4)	162(4)
C1-H1···O5 ^c	1.03(3)	2.44(3)	3.032(4)	115(2)
H bonds Involving Counterions, Solvents and Cation Layers				
O1W-H _A (O1W)···O17 ⁱ	0.84(5)	1.81(5)	2.616(4)	161(4)
O17-H(O17)···O20	0.84	1.88	2.573(6)	139
O20-H(O20)···O12 ^v	0.84	2.00	2.800(7)	160
O20-H(O20)···O11 ^v	0.84	2.64	3.353(9)	143
C8-H _c (C8)···O11	0.98	2.36	3.217(6)	145
C47-H _B (C47)···O13 ^{iv}	0.98	2.54	3.512(6)	172
C47-H _c (C47)···O12 ⁱⁱⁱ	0.98	2.44	3.339(5)	153
C23-H23···O15	0.84(4)	2.43(5)	3.198(6)	152(4)
C33-H _B (C33)···O14 ⁱⁱⁱ	0.98	2.43	3.347(7)	156
C57-H _B (C57)···O16 ^{iii,c}	0.99	2.54	3.103(8)	116
Interchain H bonds				
C20-H _c (C20)···O10 ⁱⁱ	0.98	2.44	3.256(4)	141
C15-H(C15)···O1W ^{vi}	0.99(4)	2.51(4)	3.498(4)	174(3)

^a O11, O12, O13, O14, O15 and O16 belong to the NO₃⁻ counterions; O17 and O20 belong to the lattice EtOH molecules; C8, C20, C33 and C47 are methyl carbon atoms; C1, C15 and C23 are aromatic carbon atoms; C57 belongs to a lattice EtOH molecule; all these atoms are not shown or/and labelled in Figures

3 and S19. ^b Symmetry codes: (i) $x-1, y, z$; (ii) $-x-2, -y-1, -z$; (iii) $x, y+1, z$; (iv) $-x-2, -y-1, -z-1$; (v) $x+1, y+1, z$; (vi) $-x-2, -y, -z$. ^c Due to the very small D-H \cdots A angles, these interactions may not be considered as H bonds. D = donor; A = acceptor.

Table S4. H-bonding interactions in the crystal structure of complex **4**.^{a,b}

D-H \cdots A	D-H (Å)	H \cdots A (Å)	D \cdots A (Å)	D-H \cdots A (°)
C12-H(C12) \cdots N8 ⁱⁱⁱ	0.92(3)	2.56(3)	3.314(4)	140(2)
C12-H(C12) \cdots O2 ⁱⁱⁱ	0.92(3)	2.58(3)	3.343(4)	142(2)
C17-H(C17) \cdots N4 ⁱⁱ	0.95(3)	2.37(3)	3.274(4)	160(2)
C1-H(C1) \cdots O5	0.93(3)	2.51(3)	3.202(4)	132(2)
C13-H(C13) \cdots O5 ⁱⁱ	0.96(3)	2.61(3)	3.468(4)	150(2)
C14-H(C14) \cdots O4 ⁱ	0.93(3)	2.41(3)	3.136(4)	134(2)
C7-H _A (C7) \cdots O3 ⁱ	0.96(4)	2.43(4)	3.325(4)	155(3)
C7-H _B (C7) \cdots N7 ⁱ	0.92(4)	2.62(4)	3.513(4)	166(3)

^a Atoms C1, C12, C13, C14 and C17 are aromatic carbon atoms; C17 is a methyl carbon atom; atoms O3, O4 and O5 belong to the ClO₄⁻ counter ion; all these atoms are not shown or/and labelled in Figures 5 and S20. ^b Symmetry codes: (i) $x+1, y, z$; (ii) $-x, -y+1, -z+2$; (iii) $-x+1, -y+2, -z+2$. D = donor; A = acceptor.

Table S5. H-bonding interactions in the crystal structure of complex **3**·0.8H₂O·1.3MeOH.^{a,b}

D-H \cdots A	D-H (Å)	H \cdots A (Å)	D \cdots A (Å)	D-H \cdots A (°)
C9-H(C9) \cdots O1 ⁱ	0.95	2.36	3.185(10)	145
C17-H(C17) \cdots O3 ⁱⁱ	0.95	2.40	3.248(10)	148
C22-H(C22) \cdots O9 ⁱⁱⁱ	0.95	2.49	3.188(11)	130
C24-H(C24) \cdots O5 ⁱ	0.95	2.37	3.075(14)	131
C24-H(C24) \cdots O4A ⁱ	0.95	2.53	3.44(4)	159
C25-H(C25) \cdots O6 ⁱ	0.95	2.49	3.224(17)	134
C27-H(C27) \cdots O15 ⁱⁱⁱ	0.95	2.58	3.32(4)	135
C37-H(C37) \cdots O4W	0.95	2.49	3.26(3)	139

^a Atoms C9, C17, C22, C24, C25, C27 and C37 are aromatic carbon atoms not labelled in Figures 7 and S21; O4, O5, O6, O9 and O15 belong to the ClO₄⁻ counterions not shown in Figures 7 and S21; O4W belongs to a lattice H₂O molecule not shown in Figures 7 and S21. ^b Symmetry codes: (i) $-x+1/2, -y+1/2, -z$; (ii) $-x+1, y, -z+1/2$; (iii) $x, y-1, z$. D = donor; A = acceptor.